Proceeding of the 2004 American Control Conference
Boston, Massachusetts June 30 - July 2, 2004

Dynamic Estimation for Reduced Galerkin Models of Fluid Flows

Gilead Tadmor

Electrical & Computer Engineering Department
Northeastern University
440 Dana Research Bldg., Boston, MA 02115, U.S.A.
tadmor@ece.neu.edu

Bernd R. Noack

Hermann-Föttinger-Institute of Fluid Mechanics,
Technical University of Berlin
Straße des 17 Juni 135, D-10623 Berlin, Germany
noackbr@pi.tu-berlin.de

***Abstract*— Reduced Galerkin models of fluid flows are traditionally obtained by the *Galerkin projection* of a low-dimensional flow expansion onto the the Navier-Stokes equation. A new approach in this application domain is the a posteriori model parameter estimation to correct for distortions due to the low dimensional compression. Preserving model structure, this leads to considerable improvement in dynamic prediction the cylinder wake benchmark.**

I. Introduction

Dynamic parameter estimation and adaptation need no motivation in the control community. This note is part of a relatively recent effort to extend these methods to control-oriented models and feedback design in fluid systems. Computational fluid dynamics (CFD) models strive to provide the highest resolution, with system size ranging from $O(10^4)$ states in 2D flows to $O(10^6)$ for 3D configurations. In contrast, control-oriented models emphasize the difficult balance of a drive for simplicity, necessary for practical feedback design, with the need to capture (just) enough of the relevant dynamic envelope. Possible approaches include black/gray box system ID, which worked well in relatively narrow & nearly linear regimes (e.g. [1], [2]. Linear system reduction methods [3] are applicable in some large-scale models (e.g. [4], [5]). Here physics-based reduced-order methods are used to generate an a priori very low-order model. More specifically, we focus on proper orthogonal decomposition (POD) Galerkin models, generated by of flow data [6].

According to standard procedure, the nominal POD model is obtained by compression (termed *the Galerkin projection*) of the first principles governing equation to the span of a selected set of modes in an appropriate Hilbert space (cf. §II). An unwanted side effect of the compression is the truncation and distortion of critical energy flow paths. A practiced remedy is the inclusion of a turbulence model, such as eddy viscosities [6]–[8]. Values of viscosity coefficients are commonly based on solution matching or on a priori qualitative hypotheses (e.g., a quadratic dependence on the wave number) that provide a measure of stability, but lack a rigorous mathematical justification [9], [10].

This note explores the possibility to employ parameter estimation tools to correct the reduced model parameter, using reliable CFD simulation or experimental data. Corrected parameters include energy transfer coefficients. The utility of a posteriori parameter corrections is illustrated using the cylinder wake benchmark. Indeed, it is shown that while the POD Galerkin framework is useful to determine the form and basic properties of the reduced system, drastic parameter corrections may be needed to match empirically observed system dynamics.

This paper is focused solely on modeling issues. Complementing discussions of control design with low order Galerkin models can be found e.g, in [11]–[13] by these authors.

II. Turbulence representation in Galerkin models

The development of low-dimensional Galerkin models for highly irregular turbulent flows is intimately linked to the empirical observation of large-scale coherent structures and a turbulence cascade to small-scale stochastic eddies. Coherent fluid motion can be considered as regular, low-dimensional, and deterministic. Coherent structures resolve most of the fluctuation energy and its production. In contrast, small-scale fluctuations are considered as high-dimensional and stochastic. This contribution resolves most of the enstrophy (square of the vorticity) and dissipation. The energetic coherent-structure contribution to the velocity field $\mathbf{u}$ may be captured in a low-dimensional POD Galerkin approximation,

$$\mathbf{u} = \sum_{i=0}^{N} a_i(t)\, \mathbf{u}_i(\mathbf{x}), \tag{1}$$

where $\mathbf{u}_i$, $i = 1, \ldots, N$ represent the location-dependent orthonormal POD modes, and a_i, the time-dependent Fourier coefficients. Following a notation of Rempfer [9], the mean flow $\mathbf{u}_0$ is formally included in the expansion with $a_0 \equiv 1$.

The conventional method to derive a Galerkin system, governing the temporal evolution of the Fourier coefficients, is by the Galerkin projection of (1) onto the incompressible Navier-Stokes equation. The resulting Galerkin system has the form

$$\frac{d}{dt}a_i = \nu \sum_{j=0}^{N} l_{ij}\, a_j + \sum_{j,k=0}^{N} q_{ijk}\, a_j\, a_k \quad \text{for } i = 1, \ldots, N, \tag{2}$$

with constant coefficients l_{ij} and q_{ijk}. The linear and quadratic terms represent the viscous and convective Navier-Stokes terms, respectively. Here, ν is the reciprocal of the Reynolds number Re. The pressure term may vanish, be negligible, or change the numerical values of the coefficients q_{ijk}. However, this term generally does not effect the basic form of (2) [14].

The energy-flow cascade from the resolved large scales to the neglected small scales implies that a large portion of the dissipation may not be resolved in the Galerkin system (2). Hence, the fluctuation level of the Galerkin solutions tends to be too large or even diverge. Realistic fluctuation amplitudes require a model for the energy loss. Table II summarizes the modeling task. The Galerkin approach shares this modeling task with all engineering turbulence simulations, including unsteady RANS and large eddy simulations (LES). Typically, the energy flow to the neglected small scales is modeled by adding an 'eddy' viscosity ν_t to the kinematic viscosity $\nu = 1/Re$ in the (non-dimensionalized) evolution equation. In a pioneering Galerkin

0-7803-8335-4/04/$17.00 ©2004 AACC

model of the wall turbulence [7], the linear term of (2) is replaced by $\nu_{\text{eff}} \sum_{j=0}^{N} l_{ij}\, a_j$ with an increased viscosity $\nu_{\text{eff}} := \nu + \nu_t$. Effectively, the Reynolds number is lowered to the laminar regime until the observed fluctuation level matches the level predicted by the Galerkin system. This approach is pursued in numerous other studies.

A refined turbulence representation for Galerkin models has been proposed by Rempfer [9]. In a study of transitional boundary layers, modal eddy viscosities are introduced, i.e. each POD mode has an effective viscosity $\nu_{\text{eff,i}}$ which replaces the kinematic viscosity in the i-th Galerkin system equation. This ansatz takes into account that the unresolved energy loss per unit fluctuation energy tends to increase with decreasing scale, i.e. $\nu_{\text{eff,i}}$ increases with the POD mode index i. The modal eddy viscosity may be determined by solution matching [8] or may be derived from a modal energy flow consideration [15]. The main idea of this approach is also pursued in spectral viscosities for Fourier modes (see, for instance, [6]).

properties	large scales	small scales
dimension	low-dimensional	high-dimensional
dynamics	deterministic	stochastic
level of resolution	resolved in the Galerkin approximation	modeled in the Galerkin system
kinematic role	energy	enstrophy
energetic role	production	dissipation

TABLE I
ROLE OF RESOLVED LARGE AND NON-RESOLVED SMALL SCALES

The energy-flow cascade from large to small scales is also observed in periodic [16], [14] and transitional flows [9]. In particular, the dissipative effect of the higher POD modes on the first POD modes is still intact. For instance, a Galerkin model resolving only the first harmonics with two POD modes may be improved by an eddy viscosity representing the energy-transfer term to the higher harmonics. This ansatz is pursued in the current cylinder wake study.

III. DISSIPATIVE DYNAMIC ESTIMATION

The estimator used here utilizes a quadratically dissipative structure [17], [18]. Dissipativity is commonly used in estimation and adaptation [19]. The particular form used here is motivated primarily by its simplicity, including the uncoupling of the estimation of each parameter. On a heuristic level, it also seems natural in the context of Galerkin fluid-flow models, which are directly associated with quadratic energy terms and whose structure naturally lends itself to energy-based design. This applies both to feedback control [20], parameter estimation, and eventually, adaptive control. Indeed, one advantage of the dissipative framework is the seamless modularity of the controller and the estimator, if this road map is to be followed.

The basic structure of the estimator is outlined for completeness. To simplify notations, details are provided for the estimation of diagonal parameters of the linear component of the model (e.g., the dissipation coefficients). Modifications for other configurations relevant to this note are minimal. The basic assumption is that the reduced-order model provides ample representation of its state dynamics when correct parameter values are used. A state trajectory obtained from a simulation of a reliable CFD model — or an experiment, if available — represents the correct dynamics.

The reduced Galerkin system is written in the form

$$\frac{d}{dt}\mathbf{a} = \left(L(\mathbf{a}) + d\{\sigma\}\right)\mathbf{a}. \tag{3}$$

Here, $\mathbf{a} := [a_1, \ldots, a_N]^T$ comprises the Fourier coefficients in (1). $L(\mathbf{a}) := L_0 + \sum_i^N a_i\, L_i$ is an affine matrix-valued function consisting of the coefficients in (2). The constant in (2) vanishes if the base flow $\mathbf{u}_0$ is a steady Navier-Stokes solution. Otherwise, the constant is removed by a translation to the fixed point of the Galerkin system. $\sigma := [\sigma_1, \ldots, \sigma_N]^T$ is the unknown parameter vector and the symbol "$d\{\sigma\}$" stands for the diagonal matrix defined by σ (i.e., $[d\{\sigma\}]_{kl} := \delta_{kl}\sigma_k$). Indeed, the modal eddy-viscosity ansatz of §II leads to a diagonal matrix term $d\{\nu_{\text{eff},i}\, l_{ii}\}$, realizing $[l_{ij}]$ in (2) has negligible off-diagonal terms.

The estimator is then of the form

$$\frac{d}{dt}\widehat{\mathbf{a}} = \left(L(\mathbf{a}) + d\{\widehat{\sigma}\}\right)\mathbf{a} - d\{\kappa\}\,\triangle\mathbf{a}, \tag{4a}$$

$$\frac{d}{dt}\widehat{\sigma} = d\{\mathbf{a}\}\, d\{\alpha\}^2\, \triangle\mathbf{a}, \tag{4b}$$

where $\kappa := [\kappa_1, \ldots, \kappa_N]^T$ and $\alpha := [\alpha_1, \ldots, \alpha_N]^T$ are positive design parameters, the hat '$\widehat{\ }$' indicates an estimated variable, and $\triangle$ indicates an estimation error, i.e. $\triangle\mathbf{a} := \mathbf{a} - \widehat{\mathbf{a}}$. Since correct readings of the state $\mathbf{a}(t)$ are available, so is $\triangle\mathbf{a}(t)$, enabling the simulation of the dynamic estimator (4).

Denoting the weighted error vector $\xi := [\triangle\mathbf{a}^T d\{\alpha\},\ \triangle\sigma^T]^T$, error dynamics are of the form

$$\frac{d}{dt}\xi = \begin{bmatrix} -d\{\kappa\} & d\{\mathbf{a}\}d\{\alpha\} \\ -d\{\mathbf{a}\}d\{\alpha\} & 0 \end{bmatrix} \xi. \tag{5}$$

Equivalently, for each $i = 1, \ldots, N$,

$$\frac{d}{dt}\begin{bmatrix} \alpha_i\triangle a_i \\ \triangle\sigma_i \end{bmatrix} = \begin{bmatrix} -\kappa_i & \alpha_i a_i \\ -\alpha_i a_i & 0 \end{bmatrix}\begin{bmatrix} \alpha_i\triangle a_i \\ \triangle\sigma_i \end{bmatrix}. \tag{6}$$

Each of these subsystems is dissipative with respect to the storage (Lyapunov) function $V_i = 0.5(\alpha_i^2\triangle a_i^2 + \triangle\sigma_i^2)$: $\frac{d}{dt}V_i = -\kappa_i\triangle a_i$. Drawing intuition from the standard dissipative mass–and–spring system, which is structurally similar to (6), κ_i controls dissipation and α_i controls lossless incremental energy flow from the estimation errors $\triangle\sigma_i$ to the state errors $\triangle a_i$, where it is dissipated. Quantitative parameter selection guidelines are trivial when estimation is about a nearly constant attractor, where (6) are linear time-invariant second-order systems. Clear guidelines become elusive with more complex attractors. As a general rule, κ_i needs to be balanced with α_i: a relatively large κ_i will suppress the "innovation" $\triangle a_i$ and prevent adaptation, while a relatively small value may result with undesirable oscillations. The stipulation that the nominal model structure is capable to correctly represent its own state dynamics is, at best, a good approximation. Considering in addition the inevitable measurement noise, an overly aggressive adaptation has to be avoided to prevent tracking high-frequency, unmodeled components of the measured innovation signal.

IV. MODELLING THE LAMINAR CYLINDER WAKE

The laminar vortex shedding behind a circular cylinder is used here as a benchmark example and the dynamic observers of §III are employed to improve a low-dimensional Galerkin model of this system.

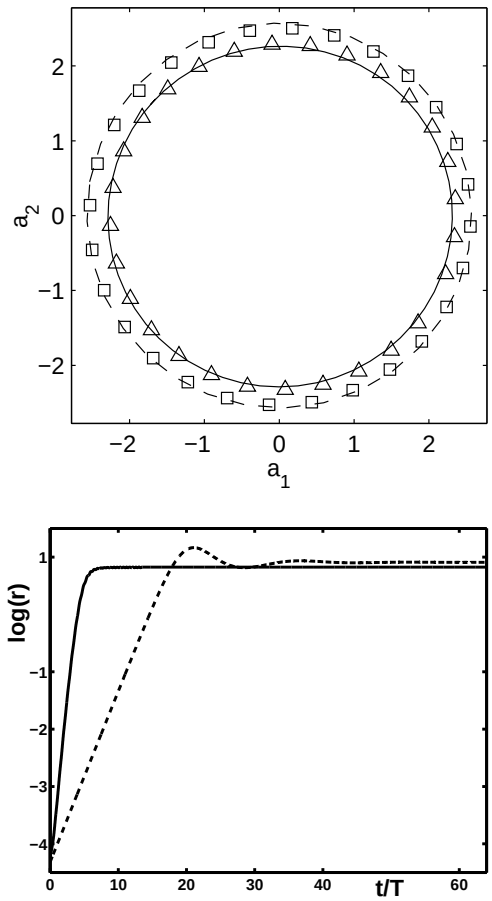

Fig. 1. Transient and attractor dynamics of a direct numerical simulation (DNS) and the original Galerkin systems. Top: Phase portrait of attractor orbits in terms of $(a_1(t), a_2(t))$. The figure displays data of DNS (solid curve), of the eight-dimensional Galerkin model (△) and of the Galerkin system (7) (□) with the original coefficients computed by the Galerkin projection. Bottom: Transient dynamics visualized in terms of $\log(r)$ from a DNS (solid curve) and from the Galerkin projection (dashed curve), demonstrating both the lower growth rate and the higher steady state value of the latter. Time is scaled with respect to the attractor's vortex shedding period T.

A. The reduced Galerkin model

The cylinder wake has been studied extensively (see, e.g., the review articles [21]–[23]). The following brief description of an empirical Galerkin model of the cylinder wake is taken from [16], where a detailed discussion of the model construction and an analysis of its properties can be found.

The system is considered at the reference Reynolds number of 100, which is far above the critical value of 47 [24] for the laminar shedding regime. The natural flow is then defined by a periodic attractor. A POD Galerkin model is obtained from a reference simulation of the attractor. As in [25], the 8-mode Galerkin approximation of the attractor accurately reproduces the simulation. These modes represent the first four vortex shedding harmonics. In fact, already the first pair captures some 96% of the perturbation kinetic energy, a very efficient representation indeed. However, a Galerkin model based on these two modes alone — essentially an ideal oscillator — is structurally unstable and lacks the means to stabilize any preferred oscillation amplitude. A shift-mode, introduced in [16], [20], provides these functions through a representation of the energy flow between the slowly varying mean flow and the leading Karhunen-Loève modes. The shift-mode is defined as the normalized difference between the mean flow of natural vortex shedding and the unstable steady Navier-Stokes solution.

A three-state Galerkin model is based on the Galerkin approximation (1) with the unstable steady Navier-Stokes solution $\mathbf{u}_s$ as the base flow, the von Kármán pair $\mathbf{u}_{1,2}$, and the shift-mode $\mathbf{u}_\Delta$ as the third mode,

$$\mathbf{u} = \mathbf{u}_s + a_1\mathbf{u}_1 + a_2\mathbf{u}_2 + a_\Delta\mathbf{u}_\Delta.$$

The Fourier coefficients a_i, $i = 1, 2$ and a_Δ define the Galerkin state space. The Galerkin projection outlined in §II leads to a Galerkin system of the form [16]

$$\frac{d}{dt}\begin{bmatrix} a_1 \\ a_2 \\ a_\Delta \end{bmatrix} = \begin{bmatrix} \sigma_o & -\omega - \gamma a_\Delta & -\beta a_1 \\ \omega + \gamma a_\Delta & \sigma_o & -\beta a_2 \\ \alpha a_1 & \alpha a_2 & -\sigma_\Delta \end{bmatrix} \begin{bmatrix} a_1 \\ a_2 \\ a_\Delta \end{bmatrix}. \tag{7}$$

An enforced phase-invariance assumption leads to multiple occurrence of the same coefficients, e.g. $\sigma_o, \omega, \alpha, \beta, \gamma$. This assumption is well obeyed numerically and can be derived analytically in the limit of spatially periodic structures. Notice that σ_o is included with a positive sign, capturing a positive net production over dissipation and energy transfer. The value of σ_Δ is included with a negative sign, capturing a net energy dissipation in the linearly uncoupled shift-mode.

A critical fact that ought to be remembered in the context of any very low order fluid flow model is that its validity dynamic envelope is inherently limited. Here, the purpose of the model is to capture the natural transients from the unstable steady flow to the attractor as depicted in Fig. 4, below. Indeed, with an appropriate actuation term added, the model can then be used to design feedback compensators for reference tracking within that envelope [20].

The Galerkin system (7) captures very transparently key ingredients of the wake flow [16]: (i) The instability of the steady flow (represented by the zero state), (ii) the dominant oscillation frequency and its dependence on changes in the mean flow, (iii) the existence of an attractive invariant manifold of transients from the neighborhood of the steady flow to the attractor, and (iv) the stability of a limit cycle attractor. However, with the parameters computed by the Galerkin projection, the model over-predicts the perturbation kinetic energy of the limit cycle ($K = 0.5(a_1^2 + a_2^2)$) and under-predicts the growth rate near the unstable steady flow. Both of these facts are visualized in Fig. 1.

The over-predicted limit cycle amplitude is explained by the truncation of the modal energy cascade in the reduced system. Indeed, already the restoration of three additional harmonics in the Galerkin model corrects this distortion [16], [25]. The fact that a POD model of the attractor is not capable to predict dynamic properties at another operating point, such as the steady flow, is not surprising. As shown in [16], a good prediction of the transient near the steady solution is obtained when the POD modes are replaced by the dominant stability eigenmodes of the Navier-Stokes equation linearized around its steady solution [24]. Our goal here is to illustrate the advantages of an a posteriori correction of the distortions caused by the Galerkin projection, using dynamic estimation. This simple example demonstrates quite dramatically

both the extent of the distortion in the a priori Galerkin projection and the feasible improvement. In fact, a model, as simple as (7), can provide a decent, if not perfect representation of the flow.

Fig. 1 reveals a clear partition of trajectories into two components: A nearly exponential growth during a finite transient, and fast transition to steady state. The estimation procedure is divided accordingly into a component relevant to the steady state, followed by an estimation of the growth rate focusing on the transients. As we use fairly clean simulation data, it could be justly argued that a static estimation (e.g. a least-mean-square procedure) may also be employed. However, the use of a dynamic procedure is justified in the larger context of more complex flows, e.g. long-term transients where the attractor cannot be characterized by a constant scalar or vector.

B. Dynamic estimation of modal dissipation

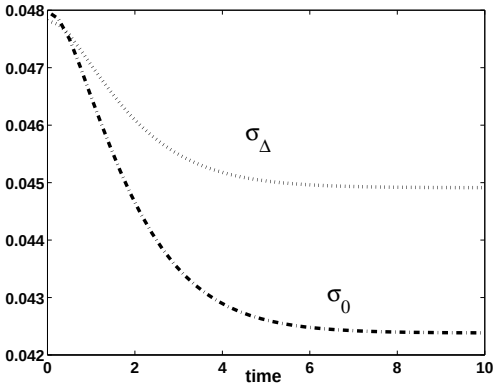

Fig. 2. Transient trajectories of $\widehat{\sigma}_o$ (dash-dots) and $\widehat{\sigma}_\Delta$ (dots).

A transition to cylindrical coordinates

$$\left[\begin{array}{c} a_1 \\ a_2 \end{array}\right] = \left[\begin{array}{c} \cos(\phi) \\ \sin(\phi) \end{array}\right] r \quad \Rightarrow \quad K = 0.5r^2, \tag{8}$$

separates energy carrying variables from phase dynamics:

$$\frac{d}{dt}\left[\begin{array}{c} r \\ a_\Delta \end{array}\right] = \left[\begin{array}{cc} \beta & 0 \\ 0 & \alpha \end{array}\right] \left[\begin{array}{cc} \frac{\sigma_o}{\beta} & -r \\ r & -\frac{\sigma_\Delta}{\alpha} \end{array}\right] \left[\begin{array}{c} r \\ a_\Delta \end{array}\right], \tag{9}$$

$$\frac{d}{dt}\phi = \omega + \gamma a_\Delta. \tag{10}$$

Evident from this form is that the attractor is determined by the values of σ_o/β and σ_Δ/α, and that the growth rates are then determined by β and α. Here, we focus on the attractor, and estimate σ_o and σ_Δ, given the nominal a priori values of β and α. The scaling factors in the matrix $d\{\beta,\, \alpha\}$ will be adjusted in a second step.

Following the general pattern of (4), the dynamic estimator is of the form:

$$\begin{array}{l} \frac{d}{dt}\left[\begin{array}{c} \widehat{r} \\ \widehat{a}_\Delta \end{array}\right] = \left[\begin{array}{cc} \widehat{\sigma}_o & -\beta r \\ \alpha r & -\widehat{\sigma}_\Delta \end{array}\right] \left[\begin{array}{c} r \\ a_\Delta \end{array}\right] + \left[\begin{array}{cc} \kappa_o & 0 \\ 0 & \kappa_\Delta \end{array}\right] \left[\begin{array}{c} \triangle r \\ \triangle a_\Delta \end{array}\right], \\ \frac{d}{dt}\left[\begin{array}{c} \widehat{\sigma}_o \\ \widehat{\sigma}_\Delta \end{array}\right] = \left[\begin{array}{cc} \alpha_o^2 r & 0 \\ 0 & -\alpha_\Delta^2 a_\Delta \end{array}\right] \left[\begin{array}{c} \triangle r \\ \triangle a_\Delta \end{array}\right]. \end{array} \tag{11}$$

Since r and a_Δ are constant over the attractor (or slowly varying under a drift in the incoming flow), eigenvalue assignment in the appropriate counterparts of (6) can be used to determine design parameter values: Selecting a desired exponential decay rate λ, we set $\kappa_o = \kappa_\Delta = 2\lambda$, $\alpha_o = \lambda/r$ and $\alpha_\Delta = \lambda/a_\Delta$. In an adaptive implementation, the selection of λ would be guided by the expected level and spectrum of measurement noise. Here, we make the arbitrary selection of $\lambda = 1$.

Nominal values of the coefficients of (7) were obtained by a Galerkin projection of the flow, normalized with respect to the cylinder diameter and incoming flow velocity (i.e., setting both to one). These values are: $\beta = 0.0190$, $\sigma_o = 0.0480$, $\sigma_\Delta = 0.0480$, $\omega = 0.9336$, $\omega_\Delta = 0.0342$, and $\alpha = 0.0196$. The limit-cycle values of the Galerkin system are $r_n = 2.4823$ and $a_{\Delta\, n} = 2.5242$. (where the subscript "n" stands for "nominal"). The steady state values from direct numerical simulation (DNS) of the Navier-Stokes equation are $r = 2.2608$ and $a_\Delta = 2.2295$. The latter are accepted as the correct values. The design coefficients are set accordingly, as $\kappa_o = \kappa_\Delta = 2$, $\alpha_o = 1/2.2608 = 0.4423$ and $\alpha_\Delta = 1/2.2295 = 0.4485$. Figure 2 depicts transient estimates of $\widehat{\sigma}_o$ and $\widehat{\sigma}_\Delta$, initiating the dynamic estimator with the correct values for $\widehat{r}$, $\widehat{a}_\Delta$, and the nominal values of σ_o and σ_Δ, for $\widehat{\sigma}_o$ and $\widehat{\sigma}_\Delta$. Indeed, the steady state values, $\widehat{\sigma}_o = 0.0424$ and $\widehat{\sigma}_\Delta = 0.0449$ are the expected values from the algebraic equalities of $\sigma_o = \beta a_\Delta$ and $\sigma_\Delta = \alpha r^2/a_\Delta$, using the DNS steady state values of r and a_Δ. Following adaptation, the attractor radius is corrected, and matches the DNS prediction as in Fig. 1.

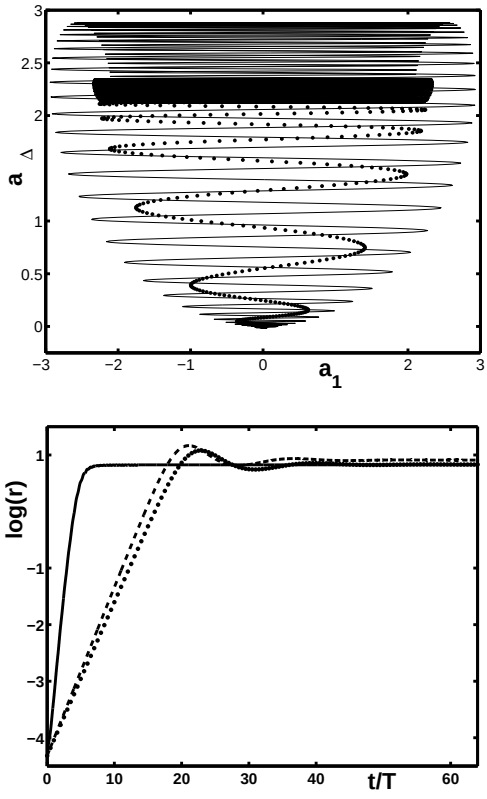

Fig. 3. Attractor calibration. Top: The attractor of DNS trajectories of (a_1, a_Δ) (dots) is matched by the corrected Galerkin system (solid), but GS transients still overshoot. Bottom: The mismatch between $\log(r)$ growth in DNS (bold) and the corrected Galerkin system (doted) is clear; as a reference, the original GS response (dashed) from Fig. 1 grows at a similar rate, as well as over-predicts the attractor.

C. Dynamic estimation of growth rates

While the corrected estimation of the energy transfer coefficients σ_o and σ_Δ resolved the issue of attractor distortion, the three states

model is still incapable to predict growth rates correctly. Fig. 3 compares a transient simulation by a DNS model with a simulation of the corrected system (7). While the two are qualitatively similar, the Galerkin system under-predicts the growth rate and supports a non-physical overshoot. In fact, the corrected lower values of σ_o and σ_Δ resulted with both a wider manifold (Fig. 3, *top*) and a lower growth rate (Fig. 3, *bottom*). The slow growth rate is a consequence of the (small) difference between the dominant oscillatory eigenmodes near the steady flow and the attractor's POD modes [16].

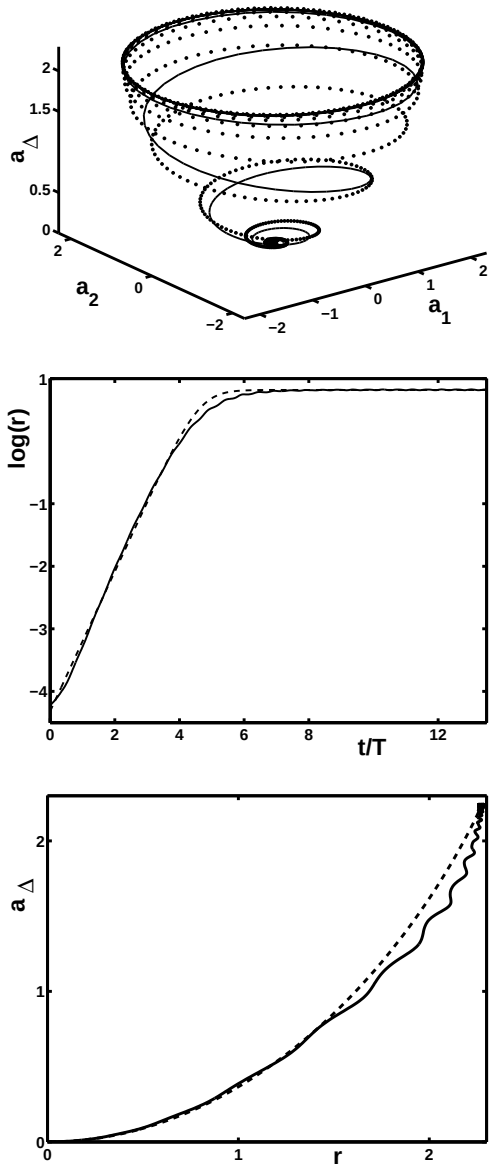

Fig. 4. Transient dynamics calibration in the Galerkin system. Top: Transient trajectories of (a_1, a_2, a_Δ) from a DNS (dots) and as predicted by the scaled Galerkin system (12) (solid line). Middle: The logarithmic perturbation growth $\log(r)$ of a DNS (bold) and of the scaled Galerkin system (dashed). Bottom: Comparison of the DNS manifold (r, a_Δ) (solid) and the Galerkin model prediction (dashed).

The adaptation in this section builds on the system structure in (9), where the vector field is defined by a cascade of two matrices, multiplying the state. The inner right matrix

$$\begin{bmatrix} \frac{\sigma_o}{\beta} & -r \\ r & -\frac{\sigma_\Delta}{\alpha} \end{bmatrix}$$

defines the attractor, and will be left fixed with its value from the previous section. The outer left matrix, $d\{\beta,\, \alpha\}$, determines the growth and convergence rates, and will be replaced by a scaling matrix $d\{\mu_o,\, \mu_\Delta\}$ that will be the subject of adaptation.

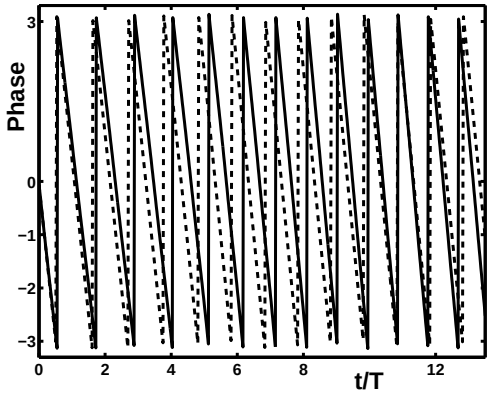

Fig. 5. Transient trajectories of $phase(a_1, a_2)$ from a DNS (solid) and as predicted by the scaled Galerkin system (dashed).

The dual challenge includes the fact that adaptation must utilize the short exponential growth section of the reference, as well as an intrinsic mismatch between the postulated model and the actual system dynamics (e.g., as represented by DNS data). The solution will be to iterate a non-aggressive adaptation procedure multiple times until the adapted variables converge to a limit. Since the subject of adaptation are exponential growth rates, the reference trajectories will be $x_r = \log(r)$ and $x_\Delta = \log(a_\Delta)$. Thus, the adaptors will be of the form

$$\begin{aligned} \tfrac{d}{dt}\begin{bmatrix} \widehat{x}_r \\ \widehat{x}_\Delta \end{bmatrix} &= \begin{bmatrix} \kappa_o & 0 \\ 0 & \kappa_\Delta \end{bmatrix}\begin{bmatrix} \triangle x_r \\ \triangle x_\Delta \end{bmatrix} \\ &\quad + \begin{bmatrix} \frac{\sigma_o}{\beta} - a_\Delta & 0 \\ 0 & \frac{r^2}{a_\Delta} - \frac{\sigma_\Delta}{\alpha} \end{bmatrix}\begin{bmatrix} \widehat{\mu}_o \\ \widehat{\mu}_\Delta \end{bmatrix}, \\ \tfrac{d}{dt}\begin{bmatrix} \widehat{\mu}_o \\ \widehat{\mu}_\Delta \end{bmatrix} &= \begin{bmatrix} \alpha_1^2\left(\frac{\sigma_o}{\beta} - a_\Delta\right) & 0 \\ 0 & \alpha_2^2\left(\frac{r^2}{a_\Delta} - \frac{\sigma_\Delta}{\alpha}\right) \end{bmatrix}\begin{bmatrix} \triangle x_r \\ \triangle x_\Delta \end{bmatrix}. \end{aligned} \tag{12}$$

Adaptation was iterated over the interval $[T, 3T]$, where, again, T is the attractor's vortex shedding period. The initial guesses for $\widehat{\mu}_o$ and $\widehat{\mu}_\Delta$ were the respective nominal values of $\beta = 0.0190$ and $\alpha = 0.0196$. In the limit, adapted values were $\mu_o = 0.081$ and $\mu_\Delta = 0.75$. That is, the basic growth rate for r is increased roughly four folds, and the convergence rate is set at about an order of magnitude larger than that, or roughly forty folds the prediction by the Galerkin projection. Fig. 4 compares the adapted model with the DNS simulations: The non-physical overshoot is removed, the geometry of the invariant manifold formed by transients is in good match with the simulation, and early growth rates are essentially identical. The corrected prediction of the Galerkin model growth rate is somewhat higher than DNS prediction, closer to the attractor, but the distortion is much smaller than in the nominal model. This small difference can be explained

by neglected nonlinearities, including the fact that the dominant expansion modes need to be modified away from the attractor [16], whereas our model uses a fixed set of modes.

V. Conclusions

The prevalent practice in physics-based reduced-order models, such as POD Galerkin models, is to rely on first principles models for parameters evaluation, that is, on the Galerkin projection. This simple example illustrates the need and utility of complementing these a priori evaluations with a posteriori dynamic estimation using relevant observed trajectories. Indeed, a posteriori dynamic estimations resulted with substantial parameter modification that help to reconcile observed behavior and the first principles model predictions vis-a-vis energy flow and dissipation. In closing, Fig. 5 shows that the prediction of the nominal model vis-a-vis phase dynamics also reveals some distortions, albeit on a much smaller scale. These distortions have been explained in [16] in terms of the need to modify dominant expansion modes near the steady flow.

Turbulence representations for Galerkin models of high-Reynolds-number flows are also expected to benefit from the dynamic observers discussed in this note. Current research of the authors indicate this opportunity.

Acknowledgments: The work has been supported by the Deutsche Forschungsgemeinschaft (DFG) under grant NO 258/1-1, by the DFG via the Collaborative Research Center (Sfb 557) "Control of complex turbulent shear flows" at the Technical University of Berlin, by the U.S. National Science Foundation under grants ECS-0136404, CCR-0208791 and INT INT-0230489, and by the DAAD program (PPP USA).

References

[1] A. Banaszuk, C.A. Jacobson, A.I. Khibnik & P.G. Mehta 1999 Linear and nonlinear analysis of controlled combustion processes. I. Linear analysis, *Proc. IEEE Conf. on Control Applications*.

[2] R. Becker, M. Garwon, C. Gutknecht, G. Bärwolff & R. King 2002 Regelung aerodynamischer Strömungen am Beispiel einer rückwärtsgewandten Stufe (transl.: control of aerodynamics flows examplified for the backward-facing step), *Automatisierungstechnik* **50**, 79–86.

[3] A.C. Antoulas & D.C. Sorensen 2001 Approximation of large-scale dynamical systems: An overview, *Int. J. Appl. Math. Comp. Sci.* **11**, 1093–1121.

[4] C.W. Rowley, T. Colonius & R.M. Murray 2004 Model reduction for compressible flows using POD and Galerkin projection, *Phys. D* **189**, 115–129.

[5] K.E. Willcox & A. Megretski 2003 Fourier model reduction for large-scale applications in computational fluid dynamics, *Proc. The eighth SIAM Conference on Applied Linear Algebra*.

[6] P. Holmes, J.L. Lumley & G. Berkooz 1998 *Turbulence, Coherent Structures, Dynamical Systems and Symmetry*, Cambridge University Press, Cambridge.

[7] N. Aubry, P. Holmes, J.L. Lumley & E. Stone 1988 The dynamics of coherent structures in the wall region of a turbulent boundary layer, *J. Fluid Mech.* **192**, 115–173.

[8] W. Cazemier, R.W.C.P. Verstappen & A.E.P. Veldman 1998 Proper orthogonal decomposition and low-dimensional models for driven cavity flows, *Phys. Fluids* **10**, 1685–1699.

[9] D. Rempfer 1991 *Kohärente Strukturen und Chaos beim laminar-turbulenten Grenzschichtumschlag (transl.: Coherent structures and chaos of the laminar-turbulent boundary-layer transition)*. PhD thesis, Fakultät Verfahrenstechnik der Universität Stuttgart (Part of this work has been published by D. Rempfer & F.H. Fazle (1994) in *J. Fluid Mech.* **260** & **275**).

[10] D. Rempfer 1995 *Empirische Eigenfunktionen und Galerkin-Projektionen zur Beschreibung des laminar-turbulenten Grenzschichtumschlags* (transl.: Empirical eigenfunctions and Galerkin projection for the description of the laminar-turbulent boundary-layer transition), Habilitation-Thesis, Fakultät für Luft- und Raumfahrttechnik, Universität Stuttgart.

[11] J. Gerhard, M. Pastoor, R. King, B. R. Noack, A. Dillmann, M. Morzyński & G. Tadmor 2003 Model-based control of vortex shedding using low-dimensional Galerkin models, *AIAA-Paper* **2003-4262**, 33rd AIAA Fluid Dynamics Conference and Exhibit.

[12] G. Tadmor, B.R. Noack, A. Dillmann, J. Gerhard, M. Pastoor, R. King & M. Morzyński 2003 Control, observation and energy regulation of wake flow instabilities, Paper **We10-4**, p. 2334–2339, *Proceedings of 42nd IEEE Conference on Decision and Control 2003*.

[13] B.R. Noack, G. Tadmor & M. Morzyński 2004 Actuation models and dissipative control in empirical Galerkin models of fluid flows, accepted in *Proceedings of the 2004 American Control Conference*.

[14] B.R. Noack, P. Papas & P.A. Monkewitz 2002 Low-dimensional Galerkin model of a laminar shear-layer. Technical Report 2002-01, Laboratoire de Mecanique des Fluides, Departement de Genie Mecanique, Ecole Polytechnique Fédérale de Lausanne, Switzerland (Part of this work has been submitted by the same authors as a manuscript to the *J. Fluid Mech.*).

[15] M. Couplet, P. Sagaut & C. Basdevant 2003 Intermodal energy transfers in a proper orthogonal decomposition–Galerkin representation of a turbulent separated flow, *J. Fluid Mech.* **491**, 275–284.

[16] B.R. Noack, K. Afanasiev, M. Morzyński, G. Tadmor & F. Thiele 2003 A hierarchy of low-dimensional models for the transient and post-transient cylinder wake, *J. Fluid Mech.* **497**, 335–363.

[17] R. Lozano, B. Brogliato, O. Egeland & B. Maschke 2000 *Dissipative Systems Analysis and Control: Theory and Applications*, Springer-Verlag, Berlin.

[18] R. Ortega, A. Loria, P.J. Nicklasson & H. Sira-Ramirez 1998 *Passivity-based Control of Euler-Lagrange Systems*, Springer-Verlag, Berlin.

[19] B.D.O. Anderson, R.R. Bitmead, C.R. Johnson Jr. P.V. Kokotović, R.L. Kosut, I.M.Y. Mareels, L. Praly, and B.D. Riedle 1986 *Stability of Adaptive Systems: Passivity and Averaging Analysis*, M.I.T. Press, Cambridge, MA, U.S.A.

[20] M. Pastoor, R. King, B.R. Noack, A. Dillmann & G. Tadmor 2002 Model-based coherent-structure control of turbulent shear flows using low-dimensional vortex models, *AIAA-Paper* **2003-4261**, *33rd AIAA Fluids Conference and Exhibit*.

[21] C.H.K. Williamson 1996 Vortex dynamics in the cylinder wake, *Annu. Rev. Fluid Mech.* **28**, 477–539.

[22] B.R. Noack 1999*a* On the flow around a circular cylinder. Part I: Laminar and transitional regime, *Z. angew. Math. Mech.* **79**, 223–226.

[23] B.R. Noack 1999*b* On the flow around a circular cylinder. Part II: Turbulent regime, *Z. angew. Math. Mech.* **79**, 227–230.

[24] M. Morzyński, K. Afanasiev & F. Thiele 1999 Solution of the eigenvalue problems resulting from global non-parallel flow stability analysis. *Comput. Meth. Appl. Mech. Enrgrg.* **169**, 161–176.

[25] A.E. Deane, I.G. Kevrekidis, G.E. Karniadakis & S.A. Orszag 1991 Low-dimensional models for complex geometry flows: Application to grooved channels and circular cylinders, *Phys. Fluids A* **3**, 2337–2354.